UCRL-ID-137632

Stability Issues in Ambient-Temperature Passive Magnetic Bearing Systems

R. F. Post

February 17, 2000

U.S. Department of Energy

Lawrence Livermore National Laboratory

DISCLAIMER

Work performed under the auspices of the U. S. Department of Energy by the University of California Lawrence Livermore National Laboratory under Contract W-7405-Eng-48.

Stability Issues in Ambient-Temperature Passive Magnetic Bearing Systems

R. F. Post
Lawrence Livermore National Laboratory

Abstract

The ambient-temperature passive magnetic bearing system developed at the Lawrence Livermore National Laboratory achieves rotor-dynamic stability by employing special combinations of levitating and stabilizing elements. These elements, energized by permanent magnet material, create the magnetic and electrodynamic forces that are required for the stable levitation of rotating systems, such as energy-storage flywheels. Stability criteria, derived from theory, describe the bearing element parameters, i.e., stiffnesses and damping coefficients, that are required both to assure stable levitation ("Earnshaw-stability"), and stability against whirl-type rotor-dynamic instabilities.

The work described in this report concerns experimental measurements and computer simulations that address some critical aspects of this overall stability problem. Experimentally, a test device was built to measure the damping coefficient of dampers that employ eddy currents induced in a metallic disc. Another test device was constructed for the purpose of measuring the displacement-dependent drag coefficient of annular permanent magnet bearing elements.

In the theoretical developments a computer code was written for the purpose of simulating the rotor-dynamics of our passive bearing systems. This code is capable of investigating rotor-dynamic stability effects for both small-amplitude transient displacements (i.e., those within the linear regime), and for large-amplitude displacements, where non-linear effects can become dominant. Under the latter conditions a bearing system that is stable for small-amplitude displacements may undergo a rapidly growing rotor-dynamic instability once a critical displacement is exceeded. A new result of the study was to demonstrate that stiffness anisotropy of the bearing elements (which can be designed into our bearing system) is strongly stabilizing, not only in the linear regime, but also in the non-linear regime.

I) Introduction

To put the experimental and theoretical work to be described in context, there follows a brief description of the Livermore passive magnetic bearing system.

The ambient-temperature passive magnetic bearing concept [1,2] developed at the Laboratory employs electrodynamic interactions to overcome the limitations imposed by Earnshaw's theorem [3]. This theorem, as it was later extended, asserts the impossibility of stably levitating an object using static magnetic fields (as, for example, the fields of permanent magnets). Our bearing systems, which are effective for stably levitating rotating systems above a low "critical speed," employ electrodynamic effects to evade Earnshaw's theorem. At rest, or at speeds below the critical speed, disengaging

mechanical bearings are used to maintain stability during this transition period. Thus there are three main component elements to our bearing system, all three of which are required to achieve Earnshaw-stable operation at operating speeds.

The first of these three components consists of axially symmetric elements, for example, pairs of annular rings of permanent magnet material, one stationary, and one rotating. These elements provide the levitating forces. However, as dictated by Earnshaw's theorem, such magnet pairs are intrinsically unstable, either for axial displacements from equilibrium (attracting pairs), or for transverse displacements and/or tilting motions (repelling pairs). In engineering parlance, all such bearing element pairs, if they have positive stiffness (restoring force, increasing with displacement) along one axis, then it follows that they must have negative stiffness (increasing destabilizing force with displacement) along another axis.

To achieve Earnshaw-stability, a new element must be introduced, one which has a sufficient positive stiffness along the appropriate axis to overcome the negative stiffness of these bearing element pairs. At the same time this new element must not introduce a degree of negative stiffness along the orthogonal axes to destabilize the system. To achieve this result we employ stabilizing elements employing electrodynamic effects. In electrodynamic systems, as opposed to magnetostatic systems, the relationships between forces and stiffnesses are not constrained by the consequences of Earnshaw's theorem.

The second one of the three major components, the stabilizer element, could be called a "Halbach stabilizer," in that it employs permanent-magnet bars arranged in the special configuration called a Halbach array [4], named after its inventor, Klaus Halbach of the Lawrence Berkeley National Laboratory. Invented by Halbach for use in particle accelerators, Halbach arrays are ideally suited for application in our passive magnetic bearing systems. They can be made in either cylindrical or planar form. Their property is that they develop a strong, localized, periodic magnetic field adjacent to their front surface, while canceling the fringing fields on the back surface. These stabilizers operate by placing the Halbach array on the rotating assembly in close proximity to a "stator" that consists of a close-packed array of shorted electrical circuits. When the Halbach array assembly rotates around the stator it induces currents in the stator circuits which create a repelling force (positive stiffness) for displacements from the centered equilibrium position. If the array pole number (number of wavelengths of the Halbach array around the circumference of the array) is large the field gradient near the surface of the array is very high. As a result the resulting positive stiffness of the stabilizer element can be large, amply sufficient to overcome the negative stiffness of the levitating magnets. Figure 1 shows, schematically, a cylindrical version of a Halbach stabilizer.

To complete the description of those elements of the passive bearing system that assure Earnshaw-stability, the third element is a mechanical bearing system (ball bearing, foil bearing, etc.) which, while engaged at zero or low rotation speeds, disengages at a low critical speed. (This same bearing could act as an emergency "touchdown" bearing during normal operation.) The critical speed is that speed at which the Halbach stabilizers,

which clearly require rotation to function, develop a sufficient positive stiffness to stabilize the overall system.

Over the period of time that the Livermore passive magnetic bearing work has been carried out most of the important issues associated with the above elements have been thoroughly addressed, both theoretically and experimentally. The issues that have not been adequately studied are those that arise in connection with rotor-dynamic instabilities. These instabilities originate from sources other than those addressed in achieving Earnshaw-stability. These other issues, namely, means for the control of rotor-dynamic instabilities, are the ones that were the subject of the studies reported here.

II) Rotor-Dynamic Issues

Rotor-dynamic instability of a magnetically levitated rotating system can arise from the presence of displacement-dependent drag or dissipation in the rotating system. There are three generically different driving sources for the instability. One of these is the bearing system itself. A second source could be aerodynamic drag forces or electrodynamic torques associated with motor or generator action. The third potential source is mechanical hysterisis within the rotor body itself [5].

The type of instability we are referring to is typically referred to as a "whirl-type" instability, in that it manifests itself as a growing eccentric whirling motion of the rotor. For the kinds or rotating systems that we are here considering, for example, fiber-composite flywheel rotors, unstable flexural modes of the kind that might be encountered in shaft-supported systems are typically not present within the operating speed range. For the cases considered here all such modes would have eigenfrequencies that lie above the highest operating speeds. The dominant unstable whirl mode therefore consists of an exponentially growing spiraling motion of the center-of-mass of the system. For this mode gyroscopic effects are such as to limit the excursions to pure translations, i.e., transverse displacements unaccompanied by tilting of the axis of rotation.

The equations of motion of the center of mass under the influence of the transverse stiffnesses of the bearing elements and the displacement-dependent drag terms have been given in a previous report [1]. They take the form of simultaneous differential equations for the x and y motions of the center-of-mass. The equations are repeated here for later use in this report.

$$M\frac{d^2x}{dt^2} = -K_x \quad x + \alpha_x \quad y - \beta\frac{dx}{dt} \tag{1}$$

$$M\frac{d^2y}{dt^2} = -K_y \quad y - \alpha_y \quad x - \beta\frac{dy}{dt} \tag{2}$$

Here K_x and K_y (Newtons/meter) , and α_x and α_y (Newtons/meter) are the stiffnesses and drag coefficients in the x and y directions, respectively, and β (Newtons-

sec./m.) is the damping coefficient for the eddy-current damper. The rotating mass is denoted by M (kg.).

In the case of isotropic stiffness and drag coefficients ($K_x = K_y = K$; $\alpha_x = \alpha_y = \alpha$), solution of the above equations yields the condition for stabilization by eddy-current dampers:

$$\beta > \frac{\alpha}{\Omega_0} \quad \text{, stable,} \quad \Omega_0 = \sqrt{\frac{K}{M}} \quad \text{radians/sec.} \tag{3}$$

In the case of anisotropic stiffness and drag coefficients, if no eddy-current dampers are employed, stabilization can still occur if the following condition is satisfied:

$$\frac{K_x}{K_y} < \left[1 - \frac{2\sqrt{\alpha_x \alpha_y}}{K_y} \right] \quad \text{, stable, } K_x < K_y \tag{4}$$

As seen from these equations there are two means by which to avoid transverse whirl instabilities, both of which - eddy-current dampers or anisotropic stiffness - can be employed in our passive bearing system as needed. Eddy-current dampers have been employed before in magnetic bearing systems, for example in the active magnetic bearings developed by Fremerey [6], however, as far as we are aware, stabilization by anisotropic stiffness has not been employed in any of the active bearing systems that have been developed to date. These systems have generally relied on their sensors and electronic feedback circuits to suppress tendencies toward whirling instability. In our case, however, we must rely on passive means for control. Fortunately, our use of Halbach array stabilizers opens up the possibility of employing stiffness anisotropy as an adjunct to eddy-current damping for whirl stabilization. By varying either the turn-to-turn spacing or the loading inductances of the stator windings, or by winding the stator on an elliptical form, anisotropy in the transverse stiffness of this element can be introduced to help in stabilizing the system. In a later section we will present results obtained from computer-modeling of the rotor dynamics that illustrate this stabilization, including stabilization in the presence of non-linear terms that otherwise would lead to a very rapidly growing instability if a critical initial displacement is exceeded.

III) Eddy-Current Dampers: Theory

The type of eddy-current damper that we have considered here is shown schematically in Figure 2. As shown in the figure the damper consists of two annular permanent magnet discs oriented in the attractive mode. These magnet discs are to be attached to and coaxial with the rotating system. Located midway between the two discs is a metal (copper or aluminum) sheet. When the magnet discs are rotating, and their axis of rotation is fixed in space, the magnetic field is constant at the disc and no eddy currents are induced. However, if the axis of rotation moves transversely the disc will be exposed to a time-varying magnetic field and eddy currents will be generated in such a way as to oppose and damp the motion in a way similar to viscous damping. It is important to note that the damper plate is stationary, while the damping magnets are rotating. If the alternative arrangement, i.e., stationary magnets and

rotating disc, were to be used, the "damper" itself would become a driving source for whirl instability.

In one of our previous reports [2] a derivation of the damping coefficient for such a damper was given, with the resulting equation for the damping coefficient:

$$\beta = \frac{\pi t}{\rho}\int B_z^2 r dr \qquad \text{(Newtons m}^{-1}\text{ sec.)} \qquad (5)$$

Here B_z (Tesla) is the z-component of the magnetic field on a plane midway between the two disc magnets, t (meters) is the thickness of the conducting sheet of metal between the magnets, and ρ (ohm-meters) is its resistivity. The derivation was made under the assumption that the inequality $t(b-a) << \delta^2$ is satisfied, where b (m.) is the outer radius of the annular magnets, a (m.) is the inner radius, and δ (m.) is the electrical skin depth at the frequency of the motion of the conducting sheet. Satisfaction of this criterion assures that the magnetic field will remain approximately constant within the conducting disc during its motion, i.e., that skin effects will be small. In the measurements to be reported the thicknesses and velocities tested were such as to span the regime (at low velocities) where this criterion was satisfied, up to higher velocities and/or greater thicknesess of the metal, where it was not satisfied, with a consequent major reduction in the value of the damping coefficient. In the design of systems using this type of eddy-current damper to control whirl instabilities it is important to take this source of non-linearity in the damping coefficient into account in order to insure that stability will be maintained over the operating range of operating speeds and displacements.

Three independent means for determining the damping coefficient of eddy-dampers of the type described here were investigated and cross-checked with each other. In a given situation whichever one of these methods is easiest to employ can be used for the design. Before describing the results from the three methods we note a relationship, one that can be derived from equation 5, that can be used to perform an indirect evaluation of the damping coefficient through a simple force measurement. We note that the integral in equation 5 is same integral that gives the attractive force between the two magnets as it is proportional to the integral of the Maxwell stress tensor across a plane midway between the two magnets . That is, the force between the magnets is given by the equation:

$$F = \frac{\pi}{\mu_0}\int B_z^2 r dr \qquad \text{(Newtons)} \qquad (6)$$

Comparing equations 5 and 6 we see that the damping coefficient can be deduced directly from a force measurement through the following relationship:

$$\beta = \left[\frac{\mu_0 t}{\rho}\right] \quad F \qquad (7)$$

The second method for determining the damping coefficient is to calculate the z-component of the magnetic field between the discs and use this result to evaluate the integral in equation 5. Such a calculation is also useful when evaluating the levitating force between annular magnets in designing other elements of the passive magnetic bearing system. The method we employed in evaluating the field was to integrate the expression for the vector potential of a loop current to create surface currents that correspond to the Amperian currents representing our permanent magnet material, and then to integrate this expression to determine the z-component of the magnetic field. The equation that was derived is given by the expression:

$$B_z(r,z) = \left[\frac{B_r}{4\pi(r/a)}\right] \int_0^{2\pi} dt \left\{ \int_z^{(z+h)} \left\{ \frac{[\,1 + (z'/a)^2 - (r/a)\mathrm{Cos}(t)]\,\mathrm{Cos}(t)}{[\,1+(z'/a)^2-2(r/a)\mathrm{Cos}(t)]^{3/2}} \right\} dz' \right\} \quad \text{(Tesla)} \qquad (8)$$

Here B_r (Tesla) is the remanent magnetic field of the permanent-magnet material, a (m.) is the radius of the magnet disc, and h (m.) is its thickness. The distance from the face of the magnet to the observation point at radius r (m.) is z(m.). The above expression gives the z-component of the magnetic field from a solid disc of magnet material. To calculate the field from an annular magnet of outer radius a and inner radius b the above expression is first evaluated for a disc of radius a and then for one for radius b, and the second result is subtracted from the first, corresponding to the removal of the core from a solid disc to produce an annular magnet.

IV) Eddy-Current Dampers: Experiment

A direct measurement of the damping coefficient was made by constructing a test rig that consisted of two annular disc magnets mounted on the end of a pivoted lever arm. The length of the lever arm between the pivot point and the center of the disc magnets was 61. cm. This lever arm rested on a load-cell (located at 30.5 cm. from the pivot point) to measure the forces arising from eddy currents induced in a rotating copper disc positioned between the magnet discs. The copper disc was much larger in diameter than the magnets, which were positioned near the outer edge of the disc. In this way the field between the magnets passed through a moving conductor whose velocity was approximately constant within the gap between the magnets, thus closely simulating the situation that would arise in a damper using the same magnets and the same thickness of

damper plate. The lever assembly was mounted on the tool post of a lathe, while the copper disc was attached to a mounting plate that was held in the lathe's chuck. The velocity of the copper surface between the two magnets was then determined from the radial position of the magnets and the rotation speed of the chuck. The latter could be varied over a sufficient range to simulate the range of velocities that might be encountered when the damper was incorporated into a passive bearing system.

The magnet discs were commercial NdFeB magnets with a nominal remanent field of 1.23 Tesla. They were 0.635 cm. in thickness, with an outer diameter of 4.45 cm. and an inner hole diameter of 1.27 cm. Several copper discs were employed, with thicknesses of 0.8 mm., 1.6 mm., 3.2 mm., and 6.4 mm. The distance between the center of each disc and the center line of the magnet discs was 15.25 cm.. To determine the velocity of the copper surface between the magnet discs. this distance was multiplied by the rotation speed of the lathe chuck in radians per second. This conversion factor (between lathe RPM and conductor velocity in meters/sec.) is: Velocity (m/sec.) = .0157 x (rotation speed in RPM). The rotation speeds varied between 45 RPM and 1800 RPM, corresponding to velocities between 0.71 m/sec. and 28.2 m/sec.

Torques on the disc caused by eddy currents were measured by taking the difference of the load-cell readings obtained when the disc was at rest and when it was spinning at a chosen speed. The measured force in Newtons was then divided by a factor of 2 to take into account the 2:1 lever ratio of the test rig. Dividing this number by the velocity of the conductor between the magnets in meters/sec. yields the damping coefficient β (Newton-sec./meter). In the data taken several different spacings between the magnets were used, to investigate the variation of the damping coefficient with magnetic field intensity.

The essential content of the measurements taken can be represented by two graphs, Figure 3 and Figure 4.

In Figure 3 the damping coefficients deduced from the measurements are plotted as a function of velocity for three different thicknesses of copper disc, with a spacing between the magnets of 13 mm. At the lowest velocities the damping coefficient is seen to vary linearly with thickness, in the manner predicted by Equation 5. However, as the velocity increases only the thinnest disc has a damping coefficient that is independent of velocity over the range covered in the experiments. The thicker discs are seen to have damping coefficients that drop rapidly with increasing velocity, corresponding to a failure to satisfy the criterion used in deriving the theory, namely that the skin depth is sufficiently large compared to the geometric mean of the disc thickness and radius.

Figure 4 illustrates another deduction from the measurements. Here the disc thickness is fixed, but the spacing between the magnets is varied. At low velocities the expected increase of damping with increased magnetic field (because of closer spacing of the magnets) is evident. However, at higher velocities the closer-spaced case shows a decay with increasing velocity, indicating a failure to satisfy the skin-depth criterion. We believe that the failure here arises from a subtler point, as follows. When the magnets are

spaced closer together the magnetic field gradient at the edges of the magnet is steepened, corresponding to increasing the frequency spectrum of the time-varying field seen by the moving conductor. This increased frequency results in a decrease in the skin depth, with a consequent progressive failure to satisfy the skin-depth criterion as the velocity increases.

The observed non-linearity of the damping coefficients as a function of velocity would need to be taken into account in the design of a bearing system. Situations could arise where the damping, though adequate to suppress rotor-dynamic instabilities for small displacements from equilibrium, would be inadequate if the velocity of the displacement was sufficiently large to lie in the non-linear regime of the damper. To put this remark in perspective, an oscillatory displacement of 1.0 mm., if associated with a frequency of 250 Hz, corresponds to a peak velocity of about 1.5 m/sec, a velocity where non-linearity is beginning to be pronounced for the thickest discs that were tested.

V) Eddy Current Dampers: Correlation with Alternative Determinations

It was noted earlier that an alternative way to determine the damping coefficient of an eddy-current damper (in its linear regime) is to measure the force between the disc magnets and insert this value into Equation 7. In the work described here such force measurements were performed. The results of these measurements, for two disc magnets of the same size as those used in the eddy-current damper measurements, are summarized in Figure 5. We may insert these results into Equation 7 in order to determine the value of the damping parameter by a second method. For example, for a spacing of 5 mm. the measured value of the attractive force is 70.8 Newtons. Taking the conductivity of copper as 1.8×10^{-8} ohm-m, and considering the example of a 0.8 mm disc, then inserting this force value into Equation 7 yields a damping coefficient $\beta = 3.95$, in reasonable agreement with the value of about 3.6 as shown on Figure 4.

The third method of determining the damping coefficient is to use the force as calculated from the vector potential expression, Equation 8, giving the z-component of the magnetic field from a disc magnet. The results from this calculation can then be inserted into Equation 6 to determine the force between the two discs. We evaluated these expressions for the case of two magnets separated by a distance of 9.53 mm., finding for the calculated force the value 44.5 Newtons. This figure compares reasonable well (i.e., within 7 percent) with the directly measured value of 41.3 Newtons. Thus values of the force calculated from Equation 8 can also be inserted into Equation 7 in order to determine the damping coefficient, in those cases where neither direct measurement nor measurement of the force and use of Equation 7 are convenient.

In summary to this point, we have demonstrated three methods of determining the damping constant of eddy-current dampers operating in the velocity range where skin effects are not important. We have also, by direct measurements, investigated the non-linear effects that arise when the assumption that the skin depth is large compared to the geometric mean of the thickness and radius of the magnet discs is not satisfied. The data determined by one or more of these methods can then be inserted, together with other

parameters, into Equations 1 and 2 in order to examine the rotor-dynamic stability of the proposed system. In the next section we will discuss numerical solutions to these equations that we have made in pursuit of this objective.

VI) Computer Simulation of Whirl Instabilities with Non-Linear Drive Terms

An important step in our program to develop practical ambient-temperature passive magnetic bearing systems is to understand the behavior of such systems, not only in the linear regimes that have been studied analytically, but also in the non-linear regimes that may arise if such systems are suddenly subjected to a large-amplitude disturbance, e.g., from seismic effects. Such cases are intractable analytically and it is necessary to employ computer simulation in order to build a base of understanding, and also to permit the design of robustly stable systems. We have developed such a code by programming Equations 1 and 2, with the inclusion of non-linear terms in the displacement-dependent drive terms (the α terms in the equations). Ryutov [7] has shown that the form these terms must take is a power series in the displacement-squared as follows:

$$\alpha = [\, \alpha_0 + \alpha_1(x^2+y^2) + \alpha_2(x^2+y^2)^2 + \ldots] \tag{9}$$

In our program we included the first and second-order terms. Higher order terms could be added, but it is felt that their inclusion is not likely to be needed in order to adequately represent realistic systems. As modified, the non-linear equations of motion that were solved numerically are given below:

$$M\frac{d^2x}{dt^2} = -K_x\, x + [\, \alpha_0 + \alpha_1(x^2+y^2)]\, y - \beta\frac{dx}{dt} \tag{10}$$

$$M\frac{d^2y}{dt^2} = -K_y\, y - [\, \alpha_0 + \alpha_1(x^2+y^2)]\, x - \beta\frac{dy}{dt} \tag{11}$$

To solve these equations they were first put into dimensionless form by making a transformation of variables and defining dimensionless constants as follows:

$$\omega_0\, t = \tau\,, \quad \omega_0^2 = \frac{\sqrt{K_x K_y}}{M}\,, \quad A = \frac{\alpha}{M\omega_0^2}\,, \quad B = \frac{\beta}{M\omega_0}\,, \quad C = (1/2)\left\{\sqrt{\frac{K_x}{K_y}} - \sqrt{\frac{K_y}{K_x}}\right\}$$

The transformed equations are now:

$$\frac{d^2x}{d\tau^2} = -(1 + C)x + Ay - B\frac{dx}{d\tau} \tag{12}$$

$$\frac{d^2y}{d\tau^2} = -(1 - C)y - Ax - B\frac{dy}{d\tau} \qquad (13)$$

In the integration of these equations when a non-linear (amplitude-dependent) term was included in A, this term was redefined as:

$$A = A_0 + A_1 [x^2 + y^2] \qquad (14)$$

In the linear (small amplitude) limit, and for isotropic stiffnesses (C = 0), the stability criterion for these equations becomes:

$$B > A, \text{ Stable} \qquad (15)$$

In the linear limit stabilization by anistropic stiffness ($C \neq 0$) is achieved (with the damping term, B, equal to zero) when the following condition is satisfied:

$$C > A, \text{ Stable} \qquad (16)$$

In the linear limit the units of the displacements are arbitrary. However, in the case that the non-linear (displacement dependent) driving terms in A are included, then the units (meters, centimeters, etc.) of the displacement will be determined by the units of the coefficients of these terms.

In investigating the behavior of the numerical solutions to Equations 12 and 13, the stability criteria (145 and (16) were found to be satisfied to high accuracy. The new information derived from these equations was associated with the presence of the displacement-dependent term, A_1, in Equation 14. For example, for a "unit circle" initial displacement (i. e., x = 1.0 and $\frac{dy}{d\tau} = 1.0$ at $\tau = 0$) then the stability boundary occurred when the damping term, B, was equal to the sum of A_0 and A_1. Figure 6 is a plot of the radial displacement of the center-of-mass, $\sqrt{x^2+y^2}$, as a function of _, for displacements slightly larger and slightly smaller than the critical displacement. The explosive growth of the instability when it is present is obvious from the plot. Further investigation of the stability boundary showed that for displacements smaller than the unit-circle displacement the boundary was defined by the sum of A_0 and the product of A_1 and the square of the displacement radius. When the initial displacements were linear, rather than circular (i.e. along the x or y axis, or at an angle), then the stability boundary moved up somewhat, going from a radial amplitude of 1.0 to an amplitude of x = y = 1.2377 (r = 1.75).

Another result of the investigations was to show the effectiveness of stiffness anisotropy in stabilizing the system, even when non-linearity is present. Figure 7 illustrates this effect. The damping coefficient, B = 0.1, and $A_0 = A_1 = .05$, so that the system was stable up to a critical displacement. In the case shown an initial

displacement x = y = 1.23779 was made, just larger than the critical displacement. With C = 0 (isotropic stiffness), a rapidly growing instability is observed. However, a value of C = .02 is sufficient to stabilize the system, as shown in the other plot.

Equations 12 and 13, when solved numerically, provide a valuable extension into the non-linear regime of the theory of the whirl instability. They should provide a means for checking the stability of proposed passive bearing systems, as follows: By measuring the stiffness and drag parameters of the elements of such systems, and then plugging these values into Equations 12 and 13 the stability boundaries of the systems could be investigated, including predictions of the displacement amplitude limits for stable operation. As our work evolves we intend to use this tool wherever it is applicable.

VII) Displacement-Dependent Drag of Bearing Elements

Some work was carried out in an attempt to measure the displacement-dependent drag coefficient of annular permanent-magnet levitating magnets. Previously, an approximate formula for this drag had been derived from simple skin-depth considerations. According to this equation the coefficient, _, should have the value:

$$- = \frac{d}{p}\left[\frac{B^2}{2m_0}\right] \qquad \text{Newtons/meter} \qquad (17)$$

Here _ (m.) is the skin-depth in the magnet material, assumed small compared to the magnet dimensions, and B (Tesla) is the strength of the magnetic field between the magnets. As an example, consider a rotation speed of 10,000 RPM for NdFeB annular magnets of the type used in the eddy-current damper measurements (Section IV). For a spacing of 5 mm. the field between them is approximately 0.16 Tesla. The resistivity of NdFeB is approximately 1.6×10^{-6} ohm-m. so that the skin depth at 10,000 RPM is approximately 4.9 cm, i.e., thicker than the magnet, thus inconsistent with the assumption made in the derivation that the skin depth is small compared to all of the magnet dimensions. If one nevertheless ignores this discrepancy and calculates _ from Equation (17), the value obtained is 160 N/m. As will be seen below this value is a gross over-estimate of the actual coefficient.

An attempt was made to measure the actual drag coefficient in a test rig that included a 10,000 RPM electrical motor driving a lower annular magnet, above which was a torsion-wire-suspended upper annular magnet. The two annular magnets were separated by a thin plastic sheet to avoid torques of aerodynamic origin. The intent was to measure the torque on the upper magnet as a function of sideways displacement of the rotating magnet, and from this measurement to deduce the value of _. Within the sensitivity of the test rig no repeatable angular deflection of the upper magnet could be observed, so that only an upper limit, 2 degrees at a lateral displacement of one magnet with respect to the other of 6.4 mm., was established. From the measured torsion constant of the suspension, about 7.0×10^{-5} Newton-meters/degree, an upper limit to the drag coefficient was calculated, at about 1.0 N/m. At a speed of 10,000 RPM the

power loss corresponding to this drag force would be about 0.15 Watt. We conclude that this particular source of displacement-dependent drag and power loss, namely that arising from the annular attracting magnet pairs, should be negligible in our passive bearing systems.

VIII) Summary and Conclusions

Some critical aspects of the rotor-dynamic stability of rotating systems supported by ambient-temperature passive magnetic bearings of the Livermore type have been studied. These include the following:

- Experimental and theoretical studies of eddy-current dampers were made that will help in their design for use in stabilizing transverse whirl modes.

- To address the problem of determining the stability of systems for which the relevant parameters, such as stiffnesses and displacement-dependent drag terms, have been measured or calculated, a computer code was written to solve the equations of motion of the center-of-mass of the system. The differential equations that were solved included non-linear terms, thus addressing situations where maintaining stability would depend on limiting the displacements below a critical value. Insight into the role of dampers and/or bearing stiffness anisotropy for stabilizing the system in the presence of non-linear effects was gained.

- An attempt was made to measure the displacement-dependent drag of two attracting annular permanent magnets. The coefficient turned out to be too small to permit other than an upper-limit determination using the test rig as it was designed.

This work was performed under the auspices of the Department of Energy by the University of California Lawrence Livermore National Laboratory under Contract W-7405-Eng-48.

Acknowledgments:

The author acknowledges with gratitude the help in the theoretical analysis and in the experiments that was rendered by D. D. Ryutov, W. H. Kent, D. L. Podesta, and M. C. Fowler.

References:

[1] R. F. Post, D.D. Ryutov, J. R. Smith, L. S. Tung, "Research on Ambient-Temperature Passive Magnetic Bearings at the Lawrence Livermore National Laboratory," Proceedings of the MAG '97 Industrial Conference and Exhibition on Magnetic Bearings, p. 168 (1997).

[2] R. F. Post, D. D. Ryutov, "Ambient-Temperature Passive Magnetic Bearings: Theory and Design Equations," R. F. Post, D. D. Ryutov, Proceedings of the Sixth International Symposium on Magnetic Bearings, p. 109 (1998)

[3] S. Earnshaw, "On the Nature of the Molecular Forces which Regulate the Constitution of the Luminiferous Ether," Trans. of the Cambridge Phil. Soc., VII. Part I, p. 97 (1839)

[4] K. Halbach, "Application of Permanent Magnets in Accelerators and Electron Storage Rings," J. App. Phys. **57**, 3605 (1985)

[5] M. J. Goodwin, "Dynamics of Rotor-Bearing Systems," p. 178, Unwin Hyman, London (1989)

[6] J. K. Fremerey, "Radial Shear Force Permanent-Magnet Bearing System with Zero-Power Axial Control and Passive Radial Damping," in Magnetic Bearings, Ed. G.Schweitzer, p. 25, Springer-Verlag (1988)

[7] D. D. Ryutov, Private Communication.

Figures:

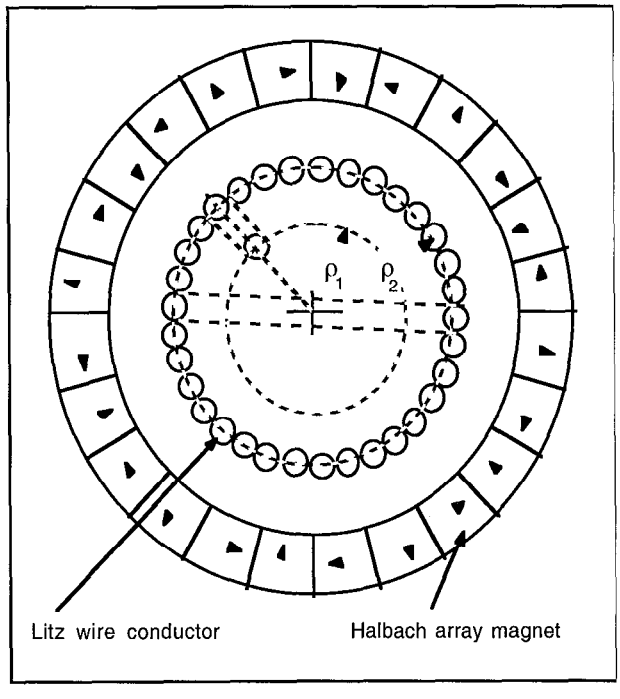

Fig. 1 Schematic drawing of Halbach stabilizer

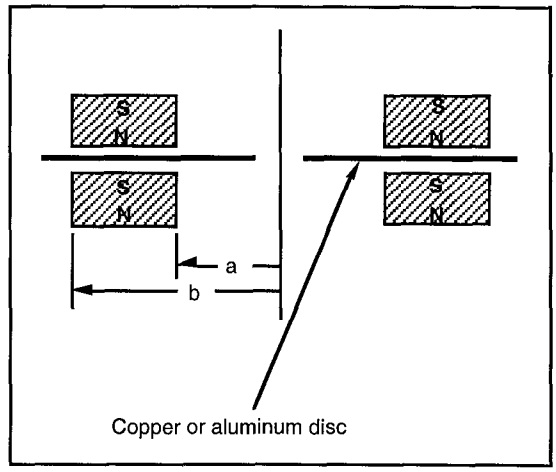

Fig. 2 Schematic drawing of eddy-current damper

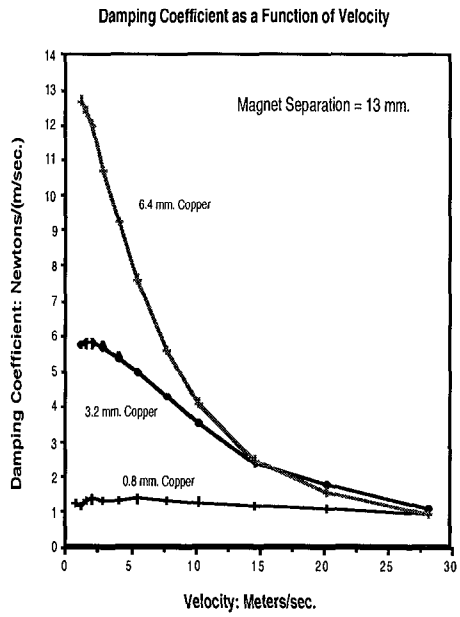

Fig. 3 Measured damping coefficient as a function of velocity for various conductor thicknesses

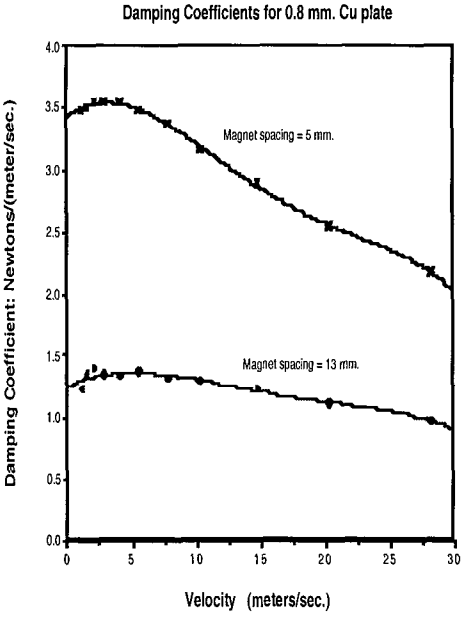

Fig. 4 Measured damping coefficient for an 0.8 mm. copper conductor as a function of magnet spacing

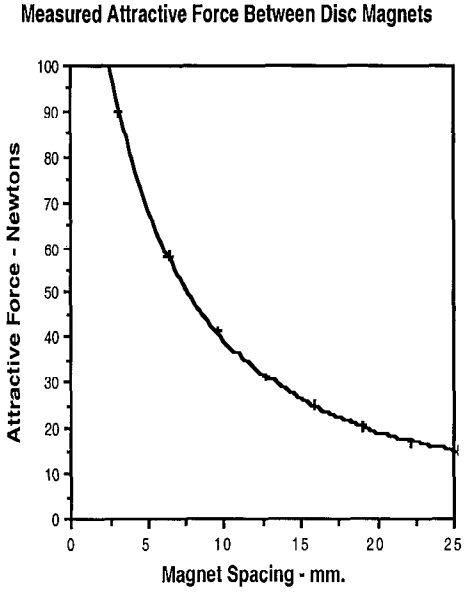

Fig. 5 Measured attractive force between annular magnets as a function of magnet spacing

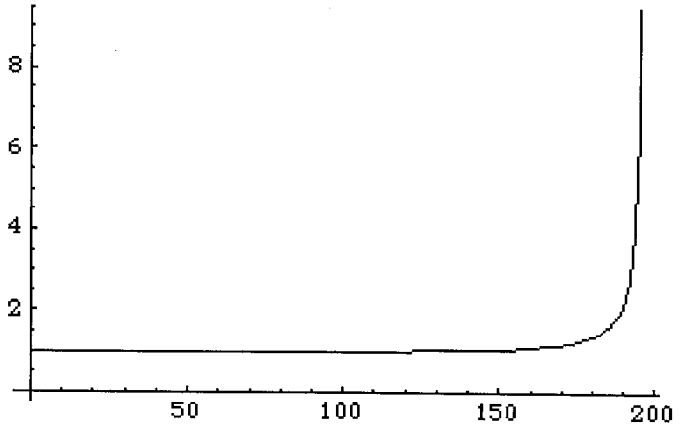

Fig. 6a Plot of the radial displacement of the center-of-mass as a function of τ for an initial circular displacement of 1.0001 units, showing onset of rapidly growing (non-linear) instability.

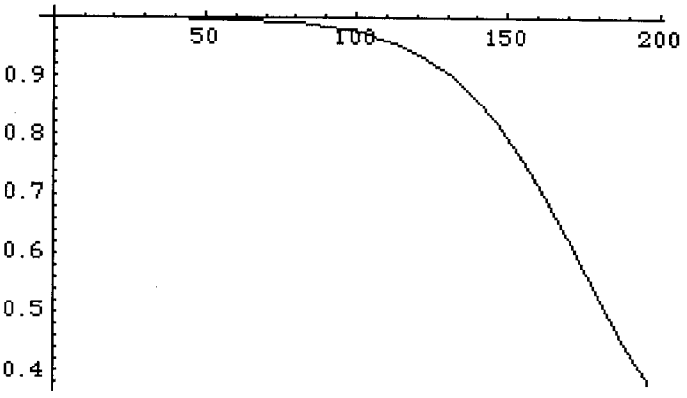

Fig. 6b Plot of the radial displacement for the same conditions as in Figure 6a, except that the initial displacement was reduced to 0.9999 units so that system remains stable (amplitude decreases with time).

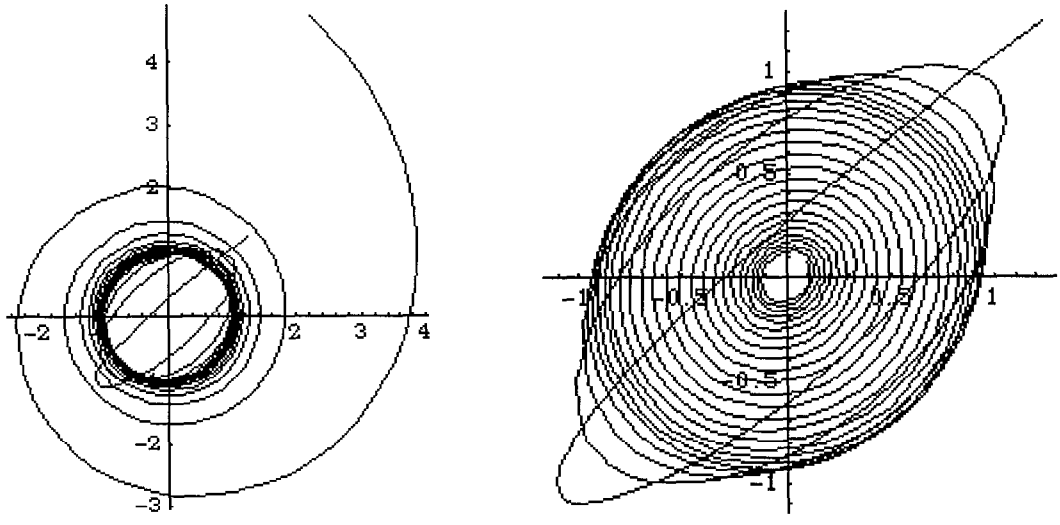

Fig. 7 Left side: Unstably growing displacement with C = 0 (isotropic stiffness) Right side: Same parameters as other plot except C = .02 (small amount of stiffness anisotropy).